JMEPEG (2010) 19:510–514
DOI: 10.1007/s11665-010-9615-3

Simulation of Tensile Behavior in Friction Stir Welded and Superplastically Formed-Titanium 6Al-4V alloy

Paul D. Edwards, Daniel G. Sanders, and M. Ramulu

(Submitted December 8, 2009; in revised form January 18, 2010)

A hybrid numerical and experimental study was undertaken to evaluate the performance of friction stir welded (FSW) and superplastically formed friction stir welded (SPF-FSW) titanium joints. This paper presents the numerical models which were developed to simulate mechanical response of FSW and SPF-FSW joints. The simulation results were compared to experimentally determined behavior characteristics of the joints to assess the validity of the modeling approach. It was found that numerical modeling have simulated successfully the tensile behavior of a FSW joint agreeing with the experimental results. This method also adequately simulated the tensile behavior of a SPF-FSW joint, but due to geometrical influences, there are discrepancies between the numerical results and experimental observations.

Keywords 6Al-4V, friction stir welding, superplastic forming, superplastically, tensile behavior, titanium

1. Introduction

Friction stir welding is a solid-state joining process. The resulting joints have the potential to be stronger and more reliable than traditional welds because there is less chance of producing voids, defects, crack, and distortions that are normally associated with solidification of fusion welds. Furthermore, the microstructure of solid-state joints is similar to that of the wrought material as opposed to the large, coarse grained, cast-type microstructures produced in fusion welds. Since its inception in 1991 (Ref 1), FSW has been used to join aluminum, magnesium, copper, and even steel (Ref 1-3).

In the FSW process, a rotating tool is plunged between the abutting faces of two materials under a vertically applied forge load and translated along the joint line, as shown schematically in Fig. 1. As the rotating tool surface contacts the workpiece under the applied forge load, an enormous amount of frictional heat is generated. This frictional heat locally softens the plasticized material to the point where the flow stress is dramatically reduced. The joint is produced by the extreme plastic deformation induced by the rotating tool in the workpiece materials. As the tool traverses along the joining line, the material heated by friction is sheared from the advancing side of the weld, moved around the pin, and deposited randomly behind the tool (Ref 3). During the process, the temperature of the weld never exceeds the melting temperature of the workpiece material (Ref 1). Therefore, there is very little chance for porosity or thermal cracking because this is a completely solid-state process.

Only recently has FSW been applied to the joining of titanium (Ref 3-9) due to difficulties of welding high-strength alloys, such as tooling material and thermal management. The titanium FSW process has sparked much interest in the aerospace industry as this process could play a major role in next generation manufacturing techniques. One such manufacturing technique where FSW will have a dramatic effect is the near net shape forming process SPF. By using FSW to join multiple sheets of titanium together, large blanks can be created for monolithic SPF operations. SPF is an advanced metal forming process which takes advantage of the metallurgical phenomenon of superplasticity (Ref 10).

Superplasticity is the ability of metallic materials to undergo large plastic strains with minimal necking and strain hardening. In the SPF process, highly complex near net shape sheet metal parts can be formed from stock sheet in a single operation. This is accomplished by placing a sheet metal blank over a die in a heated press and forcing the blank into the shape of the die under carefully controlled back pressure, as illustrated in Fig. 2 (Ref 10). SPF has been successfully applied to many materials, but it is most commonly used with aluminum and titanium in industrial applications.

Due to the microstructural characteristics of FSW titanium joints, it is possible to SPF parts containing them. Currently, there has been very little or limited research reported on the combination of these two processes in producing titanium structural components. Recently, a University-Industry collaborative FSW-SPF research was undertaken at the University of Washington. Experimental evaluations on the mechanical properties of FSW and SPF-FSW titanium joints have shown promising results (Ref 11, 12). However, to date, little has been reported on the numerical modeling of FSW titanium joint tensile behavior. Furthermore, the limited literature available on this subject has only been applied to aluminum alloys (Ref 13-15). Therefore, the purpose of this study is to present the numerical model used to simulate the mechanical behavior of FSW and SPF-FSW titanium joints.

This article is based on a presentation at the AeroMat Conference, International Symposium on Superplasticity and Superplastic Forming (SPF) held in Austin, TX, June 23-26, 2008.

Paul D. Edwards and **Daniel G. Sanders**, The University of Washington, Seattle, WA and The Boeing Company, Seattle, WA and **M. Ramulu**, The University of Washington, Seattle, WA. Contact e-mails: paul.d.edwards2@boeing.com and daniel.g.sanders@boeing.com.

2. Experimental Procedure

Extensive room temperature tensile tests were conducted to determine the global stress versus strain relationship of welded joints. All tested specimens were produced from standard Ti-6Al-4V sheet of 2.5 mm thickness. Specimens were fabricated from FSW and FSW-SPF test panels in such a way that the weld would be located in the center of the gage length. The specimens were also oriented such that the welding direction was perpendicular to the loading direction, or long dimension of the coupon as shown in Fig. 3. This facilitated evaluation of the transverse tensile properties of the weldments. Specimens were cut from welded plates using Abrasive Water Jet (AWJ) cutting and prepared into standard tensile testing coupons per ASTM E-8. Dimensions of the test coupons are shown in Fig. 3.

Tensile tests were conducted on a 250 KN capacity 5585 Instron Load Frame. Displacement control was used to failure with constant cross head extension speed of 1.27 mm/min.

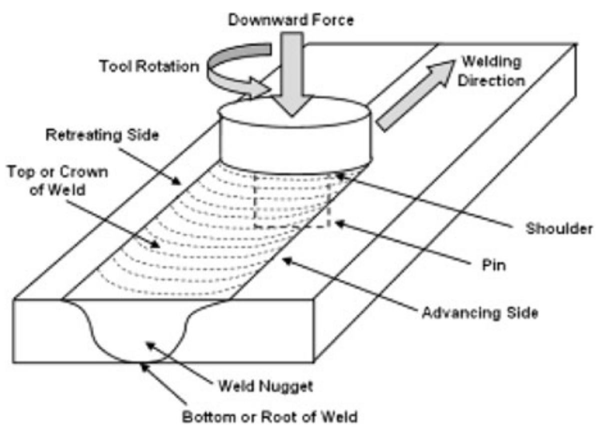

Fig. 1 Friction stir welding schematic

The applied load was monitored with a standard load cell built into the Instron Load Frame, and the displacement of the test coupon was monitored by an EIR Model LE-01 optical extensometer.

Standard Ti-6Al-4V has a yield strength of around 1103 MPa (160 ksi), an ultimate tensile strength of about 1172 MPa (170 ksi) and an elongation at failure of about 10%. On average, the as FSW specimens showed a 4% increase in yield strength, a 1% increase in ultimate tensile strength, and a 55% decrease in elongation compared to the parent material properties (Ref 12). The SPF-FSW specimens exhibited a 19% decrease in yield strength, a 21% decrease in ultimate tensile strength, and a 49% reduction in elongation on average compared to the parent material (Ref 12). Typical stress versus strain curves for FSW and FSW-SPF tests are given in Fig. 4.

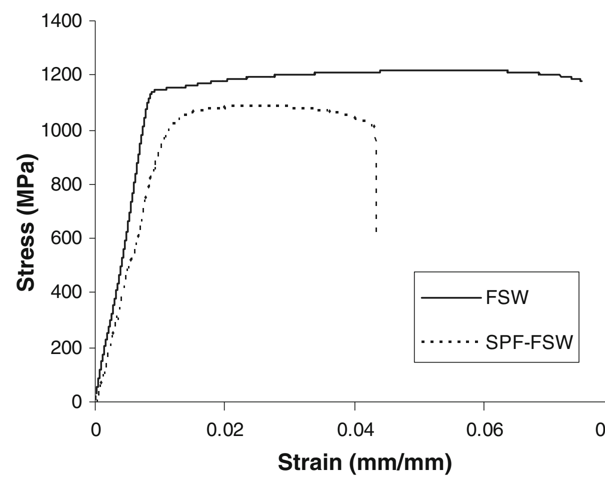

Fig. 4 Experimentally determined FSW and SPF-FSW true stress-strain curves

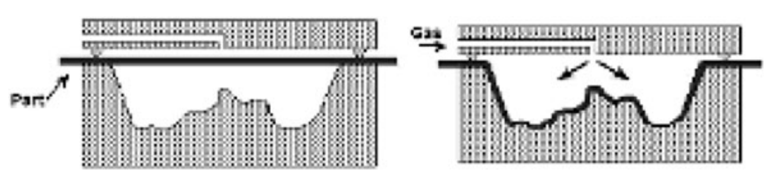

Fig. 2 SPF process schematic (Ref 10)

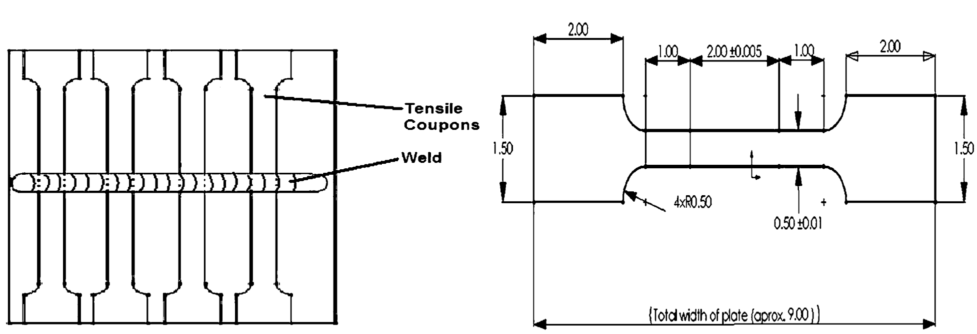

Fig. 3 Tensile coupon layout-orientation and dimensions. Weld width is ~22 mm

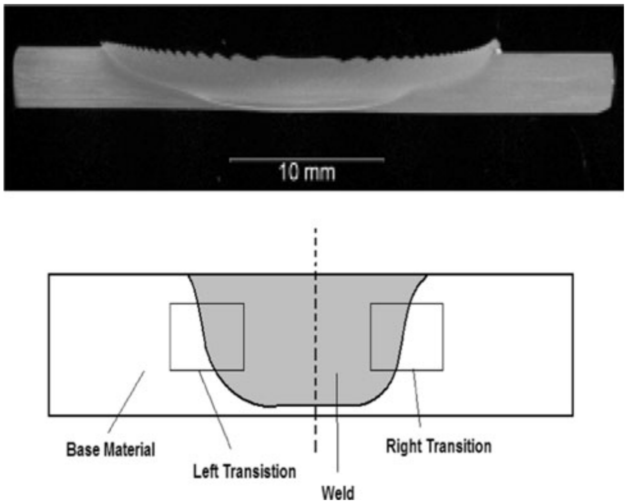

Fig. 5 Typical weld nugget cross section (*top*) and schematic (*bottom*) depicting locations from which micrographs were taken

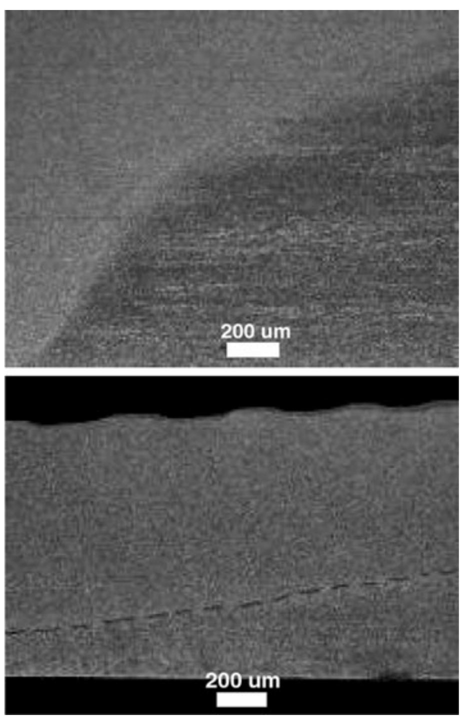

Fig. 6 Microstructures of right transitional zones in as FSW (*top*) and SPF-FSW (*bottom*) joints. The weld nugget is in the upper left corner of each picture and the base material is in the lower right. The nugget-parent material transition line is shown with a *dashed line* in the SPF-FSW picture because it is very difficult to see

In addition to mechanical property observations, the microstructural characteristics of the joints were examined. Samples were polished on a 5- and 1-μm alumina-oxide polishing wheel, and then, etched with a chemical composition of 11% HF, 33% HNO_3, and 56% de-ionized water. Figure 5 illustrates a typical titanium FSW joint sectioned surface, and the magnified microstructures are shown in Fig. 6.

Metallurgical examinations show that there is grain refinement and reorientation in the weld zone. It should also be noted that an important distinction between the microstructure of FSW aluminum and titanium is that there appears to be little or no thermo-mechanically affected zone in titanium. Instead the microstructure of the weld transitions abruptly to the undisturbed base material. This is likely due to thermal conductivity differences between the two materials.

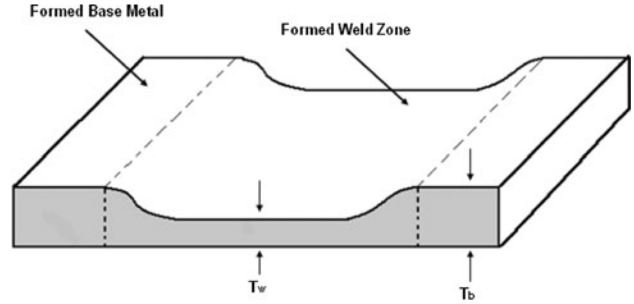

Fig. 7 Cross section schematic of SPF-FSW joint transverse to the welding direction showing the post-forming thickness differences between the base material, t_b, and the weld nugget, t_w

One substantial difference between FSW and SPF-FSW joints is that during the SPF process differences between the base material and weld microstructure and thickness can result in different straining rates in the two materials during forming. These differences in strain rates can result in thickness inconsistencies in the formed specimen, or thinning, between the base material and the weld as shown in Fig. 7. Such cross-sectional differences can cause difficulties in experimentally determining the mechanical properties of the joint.

3. Finite Element Modeling Methods and Procedures

The finite element models developed for this study were constructed to simulate the experimentally observed tensile behavior of the FSW and SPF-FSW joints.

3.1 FSW Model

To model the tensile behavior of the FSW and SPF-FSW specimens, the commercial FEA Modeling software ANSYS v.10 was used. Two-dimensional four-node quadrilateral elements capable of accounting for plasticity were implemented for these simulations. Prior research has shown that two-dimensional plane stress elements are sufficient for modeling FSW tensile specimens (Ref 13-15). After selecting an element which can appropriately simulate the behavior or these materials, the stress versus strain constitutive relations, or material models, for the materials were defined. Two material models were used, one for the base material and one for the weld zone. These material models were obtained from the experimental tensile test results for FSW and SPF-FSW titanium joints. The boundary conditions that were applied to the model were defined to simulate the loads and constraints applied to a specimen during an actual tension test.

For the FSW specimens, it is obvious that the gage length is not homogeneous due to the weld. To account for this, three different areas were created and combined to simulate the rectangular gage length of a standard tensile specimen. The first area was a 25.4 mm (1.0 in.) by 12.7 mm (0.5 in.) rectangle at the center of the gage length which would represent the weld whose properties were determined by an extensometer with a 25.4-mm (1.0 in.) gage length. The other two areas were 12.7 mm (0.5 in.) by 44.45 mm (1.75 in.) rectangles on either side of the center rectangle to represent the rest of the base metal gage length. These three areas were then glued together and meshed to form the composite material model as illustrated in Fig. 8.

Once the model had been created, meshed with elements, and the boundary conditions applied, the simulation was run. The analysis was carried out over an incremental time step of 0.01 starting at time zero and running until a time of unity was reached. Iterations were performed using various specified displacement boundary condition values until a converged solution was achieved.

3.2 SPF-FSW Model

As described in the experimental results section, the cross section of the SPF-FSW welds change during SPF. This will not only make it difficult to experimentally determine the stress-strain relationship in the weld, but it also complicates the modeling and simulation process. A two-dimensional model representing the side of the SPF-FSW tensile specimen was developed to examine the effects of thinning in the weld region on joint properties. The modeling methods used in the FSW model, including the boundary conditions, were also used in the SPF-FSW model, except for the material properties and the specimen geometry. The geometry used in the SPF-FSW model was representative of a typical SPF-FSW specimen which had undergone substantial thinning in the weld region. The model for the SPF-FSW tensile specimen is shown in Fig. 9.

4. Results and Discussion

Finite element analyses were performed for each weld case. Upon performing each simulation, stress and strain data were extracted at various time steps and plotted as a stress versus strain curve. This curve was then compared with the experimentally determined stress-strain plots. Stresses were found by averaging the equivalent stresses at five points across the width of the weld. Strain values were computed by finding the displacements of two nodes 12.7 mm (0.5 in.) to either side of the weld centerline to compare with the strain that was measured by the extensometer during experiments.

Stress distributions in the modeled tensile specimen can also be determined in the ANSYS post processor. Nodal solution contour plots of the equivalent stresses in the loading direction can be found in order to gain insight into the stress distributions induced in the joints. This is especially important for the SPF-FSW condition as the thinning effect is expected to have an interesting effect. The contour plots are for insight purposes only, and show the nature of the stress distributions. They are not meant to be used for quantitative purposes as corresponding numerical scales have not been included.

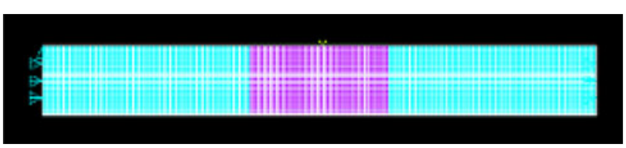

Fig. 8 Constrained and meshed bi-material model. *Light areas* show base material area and *dark central* region is the FSW material. Model is constrained on the left edge and incrementally displaced along the right edge

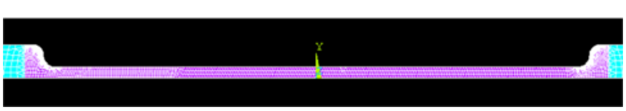

Fig. 9 SPF-FSW model showing the thinned FSW cross section within a SPF tensile specimen

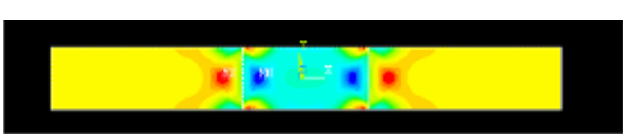

Fig. 10 First principal stress distribution in FSW bi-material model

4.1 FSW Simulations

A typical stress distribution produced by the FSW material model is shown using a contour plot (Fig. 10). The resulting stress-strain curves from the model are compared to the experimentally determined curve in Fig. 11.

The correlation between numerical and experimental results was strong. However, the stresses computed by the model are slightly lower than those found experimentally. This may arise as a result of the constant thickness assumption in the model. In reality, the base material may have actually been slightly thicker than the weld zone. Otherwise, this two-dimensional modeling method appears to be a valid way of simulating the mechanical behavior of a FSW joint.

4.2 SPF-FSW Simulation

The first principal stress distribution and the stress versus strain response found for the SPF-FSW model compared to experimentally determined joint behavior are shown in Fig. 12 and 13.

These results show that there is a discrepancy in the elastic region of the experimental and numerical results. The elastic modulus predicted by the model is 58.3 GPa, which is 41% lower than the experimentally determined modulus. Additionally, the stress and strain at yield predicted by the model are 825 MPa and 0.014 mm/mm, respectively. This represents a 3.3% decrease in strength and a 64% increase in elongation

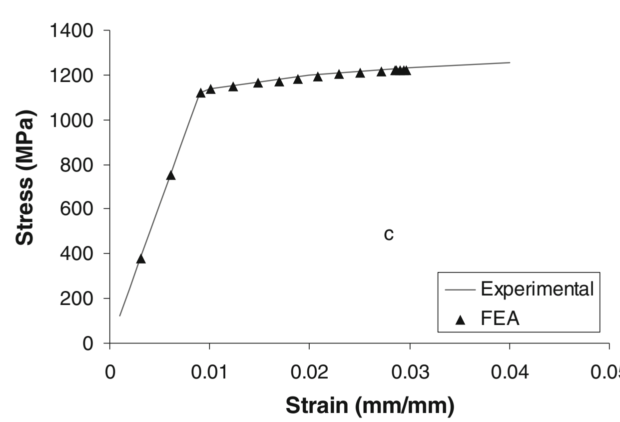

Fig. 11 FSW stress-strain curves

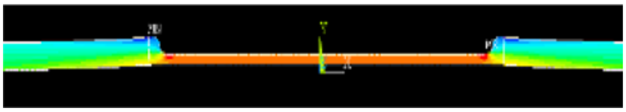

Fig. 12 First principal stress distribution for the SPF-FSW model

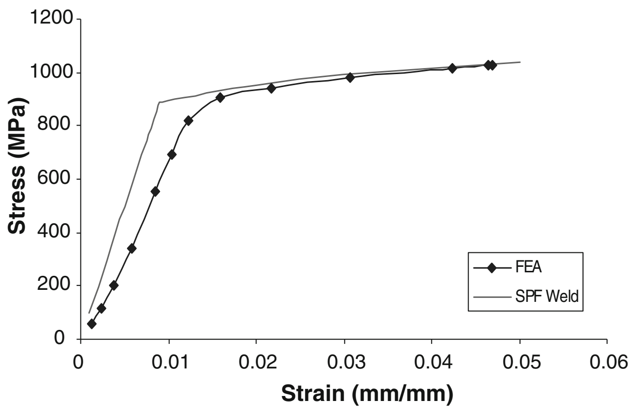

Fig. 13 SPF-FSW stress-strain results comparison

compared to the experimental results. These differences are due to effects of stress concentrations at the transitions from parent to weld material, which interfere with the stress distributions during the elastic region of the stress strain behavior. However, when the behavior becomes plastic, or nonlinear, the stresses in the weld are able to redistribute and become constant throughout the weld zone.

The results of the SPF-FSFW simulations illustrate some important points. There is definitely an effect due to thinning in the weld on experimentally determined material properties. The stress concentrations cause stress redistribution in the linear elastic region which violate the uniform stress assumption made when computing experimental stress values. Therefore, testing specimens with varying cross sections, and assuming a constant cross section, will obviously lead to inaccurate results. However, during plastic deformation the stresses can redistribute, and this minimizes the stress concentration effect and produces fairly accurate results.

In order to produce more accurate simulations of the tensile behavior of SPF-FSW joints, tensile tests should be repeated with constant gage section thickness. This would eliminate stress concentration effects when experimentally determining the stress-strain relationship of the welded joint. At this point, the modeling procedure used for simulating the tensile behavior of FSW joints could be directly applied to SPF-FSW joints and the experimental results would agree with the numerical simulations.

5. Summary

The preliminary results of the numerical models presented in this paper have verified the methodology for simulating a FSW joint and demonstrated the effect of thinning on SPF-FSW joint tensile behavior. The FSW model produced excellent agreement between simulated and experimentally determined stress-strain behavior of a FSW butt joint. However, the SPF-FSW simulation shows that thinning in the weld region from the SPF process has a significant effect on the stress-strain behavior below the yield strength. It was found that the SPF-induced thinning created stress concentrations which influence experimental determination of joint mechanical properties.

For future work, tensile properties of FSW and SPF-FSW joints should be evaluated from specimens with constant cross sections. This will eliminate the effect of gage dimensional changes on the data used in simulations. Additionally, Moire interferometric techniques should be used to determine localized strain distributions across the top surface of the weld and through the thickness. This will enable the construction of a far more detailed model to simulate the mechanical performance of these joints.

Acknowledgments

The authors of this paper would like to thank the Boeing Company for their support throughout this research project. Thanks are extended to the Edison Welding Institute and the University of South Carolina for providing the welded specimens.

References

1. The Welding Institute, 20 February 2006, <http://www.twi.co.uk/j32k/unprotected/band_1/fswintro.html>
2. R.S. Mishra and Z.Y. Ma, Friction Stir Welding and Processing, *Mater. Sci. Eng. R*, 2005, **50**, p 1–78
3. T.J. Lienert, Microstructure and Mechanical Properties of Friction Stir Welded Titanium Alloys, Chapter 7, *Friction Stir Welding and Processing*, ASM International, 2007, p 123–154. ISBN 13: 978-0-87170-840-3
4. M. Peel, A. Steuwer, M. Preuss, and P.J. Withers, Microstructure, Mechanical Properties and Residual Stresses as a Function of Welding Speed in Aluminum AA5083 Friction Stir Welds, *Acta Mater.*, 2003, **51**, p 4791–4801
5. Y. Li, E. Hood, W. Tang, and A.P. Reynolds, Friction Stir Welding of TIMETAL 21S, *Proceedings of TMS Annual Meeting*, 2005, p 81–89
6. A.J. Ramirez and M.C. Juhas, Microstructural Evolution in Ti-6Al-4V Friction Stir Welds, *Mater. Sci. Forum*, 2003, **426–432**, p 2999–3004
7. W.-B. Lee, C.-Y. Lee, W.-S. Chang, Y.-M. Yeon, and S.-B. Jung, Microstructural investigation of friction stir welded pure titanium, *Mater. Lett.*, 2005, **59**, p 3315–3318
8. A.P. Reynolds, E. Hood, and W. Tang, Texture in Friction Stir Welds of Timetal 21S, *Scripta Mater.*, 2005, **52**, p 491–494
9. T. Trapp, E. Helder, and P.R. Subramanian, FSW of Titanium Alloys for Aircraft Engine Components, *TMS Annual Meeting, Friction Stir Welding and Processing II*, 2003, p 173–178
10. D.G. Sanders and M. Ramulu, Examination of Superplastic Forming Combined with Diffusion Bonding for Titanium: Perspective from Experience, *J. Mater. Eng. Perform.*, 2004, **13**(6), p 744–752
11. E.J. Klock-McCook, "Characterization of Friction Stir Welded and Superplasticly Formed Friction Stir Welded Joints of Titanium," Masters Thesis, University of Washington, 2005
12. P.D. Edwards, "Experimental and Numerical Characterization of Friction Stir Welded and Superplastically Formed Friction Stir Welded Titanium," Masters Thesis, University of Washington, 2006
13. W.D. Lockwood, B. Tomaz, and A.P. Reynolds, Mechanical Response of Friction Stir Welded AA2024: Experiment and Modeling, *Mater. Sci. Eng.*, 2002, **A323**, p 348–353
14. W.D. Lockwood and A.P. Reynolds, Simulation of the Global Response of a Friction Stir Weld Using Local Constitutive Behavior, *Mater. Sci. Eng.*, 2003, **A339**, p 35–42
15. C. Genevois, A. Deschamps, and P. Vacher, Comparative Study on Local and Global Mechanical Properties of 2024-T351, 2024-T6 and 5251-O Friction Stir Welds, *Mater. Sci. Eng. A*, 2006, **415**, p 162–170